

Electrocatalytic oxidation of quinine sulfate at a multiwall carbon nanotubes-ionic liquid modified glassy carbon electrode and its electrochemical determination

Xue-Mei Zhan · Li-Hong Liu · Zuo-Ning Gao

Received: 27 November 2009 / Revised: 4 June 2010 / Accepted: 9 August 2010 / Published online: 14 September 2010
© Springer-Verlag 2010

Abstract The electrocatalytic oxidation of quinine sulfate (QS) was investigated at a glassy carbon electrode, modified by a gel containing multiwall carbon nanotubes (MWCNTs) and room-temperature ionic liquid of 1-Butyl-3-methylimidazolium hexafluorophate (BMIMPF₆) in 0.10 M of phosphate buffer solution (PBS, pH 6.8). It was found that an irreversible anodic oxidation peak of QS with E_{pa} as 0.99 V appeared at MWCNTs-RTIL/glassy carbon electrode (GCE). The electrode reaction process was a diffusion-controlled one and the electrochemical oxidation involved two electrons transferring and two protons participation. Furthermore, the charge-transfer coefficient (α), diffusion coefficient (D), and electrode reaction rate constant (k_f) of QS were found to be 0.87, $7.89 \times 10^{-3} \text{ cm}^2 \cdot \text{s}^{-1}$ and $3.43 \times 10^{-2} \text{ s}^{-1}$, respectively. Under optimized conditions, linear calibration curves were obtained over the QS concentration range 3.0×10^{-6} to $1.0 \times 10^{-4} \text{ M}$ by square wave voltammetry, and the detection limit was found to be 0.44 μM based on the signal-to-noise ratio of 3. In addition, the novel MWCNTs-RTIL/GCE was characterized by the electrochemical impedance spectroscopy and the proposed method has been successfully applied in the electrochemical quantitative determination of quinine content in commercial injection samples and the determination results could meet the requirement.

Keywords Quinine sulfate · MWCNTs-RTIL/GCE · Electrocatalytic oxidation · Electrochemical determination

Introduction

Since the discovery of carbon nanotubes (CNTs) by Iijima [1] in 1991 using transmission electron microscopy, CNTs have been the subject of various investigations in chemical, physical, and material areas due to its special structure, mechanical, electronic, and chemical properties [2, 3]. Depending on their atomic structure, CNTs behave electrically either as a metal or a semiconductor [4, 5]. Their subtle electronic properties suggest that CNTs have the ability to promote charge-transfer reactions when used as electrode-modifying materials [6–10].

Room temperature ionic liquids (RTILs) are compounds consisting entirely of ions that exist in the liquid state around room temperature [11, 12]. As the green reaction solvents in fundamental research and applications, RTILs have good chemical and physical properties such as good chemical and thermal stability, negligible vapor pressure, high conductivity, good biocompatibility, low toxicity, and a wide electrochemical window [13–18]. Fukushima et al. [19] easily made single wall carbon nanotubes-ionic liquid (SWNTs-IL) gels modified electrode based on the high viscosity of the IL and the “cation- π ” interactions of RTILs and CNTs. The gels is made by grinding the mixture of imidazolium ion-based RTIL and pristine single-walled CNTs. Zhao et al. [20] developed a novel modified electrode used a gel containing multiwalled CNTs and RTIL of 1-butyl-3-methylimidazolium hexafluorophosphate (BMIMPF₆) for the direct electrochemical determination of proteins, and demonstrated such gel modified electrode was thermally stable with high conductivity. Zeng’ group [21] dicussed the improved voltammetric response of l-tyrosine on multi-walled CNTs-IL composite coated glassy carbon electrodes in the presence of cupric ion. Dong’ group [22] reported the electrochemical characteristics of glucose

X.-M. Zhan · L.-H. Liu · Z.-N. Gao (✉)
Key Laboratory of Energy Sources and Chemical Engineering,
College of Chemistry and Chemical Engineering,
Ningxia University,
Yinchuan 750021, People’s Republic of China
e-mail: gaozn@nxu.edu.cn

oxidase adsorbed at CNTs modified electrode with IL as binder. Thus, the combination of the RTILs and CNTs can get a favorable fabrication of modified electrode which can be successfully applied in electrocatalysis of bioelectrochemical reaction, fabrication of biosensors, and detecting various biomolecules.

Quinine (QN), a kind of alkaloid extracted from Peruvian bark by two French chemists (P. Jpelletier and J. Bcaventou) in year 1820, was first used to treat malaria in Rome in 1631, its anti-malarial reaction mechanism is that steady deoxyribonucleic acid (DNA)-quinine compound is formed from the interaction of quinine and DNA in plasmodium, and then prevents plasmodium DNA replication and ribonucleic acid transcription; accordingly, it makes curative effects. In recent years, QN is widely used in industry, pharmacology, biochemistry, and so on. Firstly, due to the four chiral centers (carbon atoms in the third, fourth, eighth, and ninth position as shown in Fig. 1) in the molecule, QN can act as a chiral ligand and catalyst in anisomeric synthesis [23]. Secondly, quinine hydrochloride or sulfate has been utilized extensively in the cosmetics industry (shampoo) and the soft drinks especially as a flavoring agent [24]. Moreover, QN also has analgesic, antiseptic, and the muscle-relaxant properties, which was found effective as additional therapy for acquired immune deficiency syndrome [25], neurodermatitis, perennial rhinitis, and other viral diseases [26, 27]. In addition, QN has also a side-effect on intestine, stomach, and nerve centralis; if taken excessively, it even brings hypersusceptibility [28]. From what is mentioned above, various techniques have been developed for the quantitative determination of QN in beverage, plasma, human urine, biological fluids, or drugs including non-aqueous titration [28], chemiluminescence [29, 30], isotachopheresis [31], fluorodensitometric [32] and fluorimetry [33–35], direct [36, 37] and indirect [38–

40] photometry and chromatography [41–48]. Besides, a few electrochemical techniques, involving polarography, potentiometry with polymer membrane-based ion-selective electrodes, flow injection analysis and voltammetry, have been reported. Thomas et al. [49] have investigated the kinetics of the adsorption–desorption process of quinine at the mercury electrode by the polarographic double-potential programs. Kobayashi et al. [50] have described two electroanalytical techniques of quinine on measuring the change in trans-Au nanotubules membrane current when the quinine is added to the nanotubule with inside diameters approaching molecular dimensions and detecting the change in membrane potential. Li et al. [51] have prepared polyvinyl chloride membrane quinine selective electrode and applied it in the determination of quinine in quinine hydrochloride. Zareh et al. [52] easily prepared poly(vinyl chloride) membranes based on lipophilic derivatives of tetraphenyl borate for the determination of quinine in soft drinks and verified the result by a spectrophotometric technique. Saad et al. [53] demonstrated a flow injection analysis based on polyvinyl chloride membranes for the quinine in beverages; Our group has investigated the voltammetry for quinine at sodium dodecyl benzenesulfonate and N-Butylpyridinium hexafluorophosphate ([Bupy] PF₆)-modified carbon paste electrode [54]. However, the electrocatalytic oxidation and electroanalysis of quinine sulfate (QS) at multi-wall carbon nanotubes-ionic liquid gel modified glass carbon electrode (MWCNTs-RTIL/GCE) has not been reported in the literature to the best of our knowledge.

As a continuation of our previous work [54–57], we found that the oxidation peak potential of QS at MWCNTs-RTIL/GCE slightly shifted to negative and the peak current increased by almost two times in contrast to that at MWCNTs/GCE and ten times in contrast to that at bare GCE which indicated MWCNTs-RTIL can catalyze QS electrochemical oxidation reaction very well. Moreover, the influence of experimental conditions on the electrocatalytic oxidation was investigated, the electrochemical kinetic parameters were also determined, and the electrochemical quantitative determination of QN at MWCNTs-RTIL/GCE in commercial injection samples was conducted. Compare with the reported results [28–53], the fabrication of MWCNTs-RTIL/GCE is simple, easy and stable. The procedure for the determination of QN is rapid, inexpensive, pollution-free, and requires no sample pretreatment or any time-consuming derivatization reaction and deposition steps. Although the minimum detectability, sensitivity, and accuracy of the proposed method may be not as good as photometry and chromatography [36–48] in the determination of QN in complicated samples, it is believed that it could still be as an alternative in quinine determination in commercial pharmaceutical preparation.

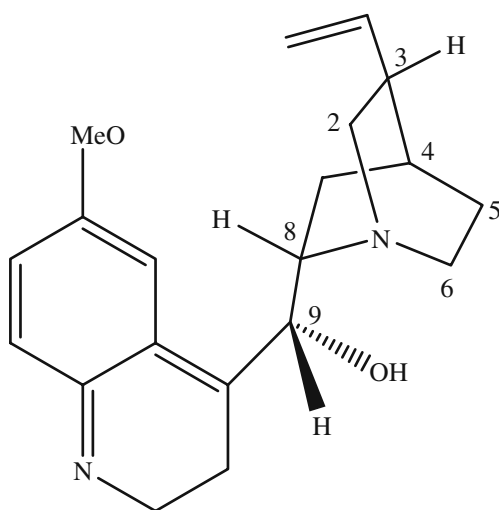


Fig. 1 Structure of quinine

Experimental

Apparatus

All electrochemical experiments were carried out using an Electrochemistry Workstation CHI660A (CH Instrument, USA). A personal computer was used for data storage and processing. The working electrodes used in cyclic voltammetry experiments were a CHI104 GCE with 3 mm diameter and GCE modified by MWCNTs and room temperature ionic liquid (MWCNTs-RTIL/GCE). A platinum wire and a saturated calomel electrode (SCE) served as the auxiliary and reference electrodes, respectively. All potentials measured and reported in this work were versus a SCE.

Reagents

Quinine sulfate (Batch No. WS20090105, Purity 99%), was from China National Medicines Chemical Reagent Ltd. and used without further purification. Quinine dihydrochloride injection (Batch No. 081201-4; labeled values of $250 \text{ mg}\cdot\text{mL}^{-1}$) was from ZhangFeng Pharmaceutical Factory (Longchuan, Yunnan Province, China). BMIMPF₆ (Shanghai Chengjie Chemical Co. Ltd, China; Purity 99%). MWCNTs (provided from Prof. Fei Wei, Chemical Engineering College of Tsinghua University, China) were functionalized to give carboxylic carbon nanotubes following the procedure [58].

Unless otherwise stated, a 0.10 M Na₂HPO₄-NaH₂PO₄ buffer solution (PBS, pH 6.8) was used as the supporting electrolyte. All other chemicals were of analytical grade and also used as received. All solutions were prepared by doubly distilled water and thoroughly flushed with high purity nitrogen that was used to remove oxygen from the solutions in the electrochemical cell. All experiments were carried out at room temperature.

Fabrication of modified electrodes

A glassy carbon electrode was polished with 0.3 μm α-Al₂O₃ slurry on the polishing micro-cloth, rinsed thoroughly with distilled water and ultrasonically successively in acetone and doubly distilled water for 10 min to remove any remaining polishing alumina.

One milligram of functionalized MWCNTs were dispersed into 2 mL of N,N-dimethyl formamide/H₂O (1:1) aqueous solution with the aid of ultrasonic stirring for 15 min to give a $0.50 \text{ mg}\cdot\text{mL}^{-1}$ homogeneous black suspension, and then 11 μL of MWCNTs dispersion was dropped on GCE surface with a microsyringe and the solvent was evaporated under infrared lamp to obtain MWCNTs/GCE. 12 mg of MWCNTs mixed with 200 μL

of BMIMPF₆ was ground for about 20 min in a mortar to give a viscous CNTs-IL gel, and then a proper amount of the gel was transferred on the cleaned electrode surface by mechanically rubbing, thus the MWCNTs-RTIL/GCE was fabricated.

Results and discussion

The electrochemical impedance spectroscopy of the bare GCE and the modified electrodes

The electrochemical impedance spectroscopy can generally provide useful information on the impedance changes of the electrode surface during the fabrication process [59]. By using Fe(CN)₆^{3-/4-}, redox couples as a electrochemical probe, the Nyquist plots of the different electrodes were shown in the curves of Fig. 2 with the frequencies range from 1 Hz to 100 kHz. It was found from the curves in Fig. 2 that the interfacial electron transfer resistance was nearly zero at MWCNTs/GCE, which indicates that the MWCNTs formed high electron conduction pathways between the electrode and electrolyte [60]. At high frequencies near the origin, MWCNTs-RTIL/GCE represented an obvious smaller semicircle than that of the bare GCE and RTIL/GCE which related to a good ionic conductivity and the least charge-transfer resistance of MWCNTs-RTIL/GCE. At low frequencies, MWCNTs-RTIL/GCE represented a linear tail with a maximal slope among the different electrodes which indicated MWCNTs-RTIL/GCE obviously improved the diffusion of ferricyanide toward the electrode surface according to the reference [61].

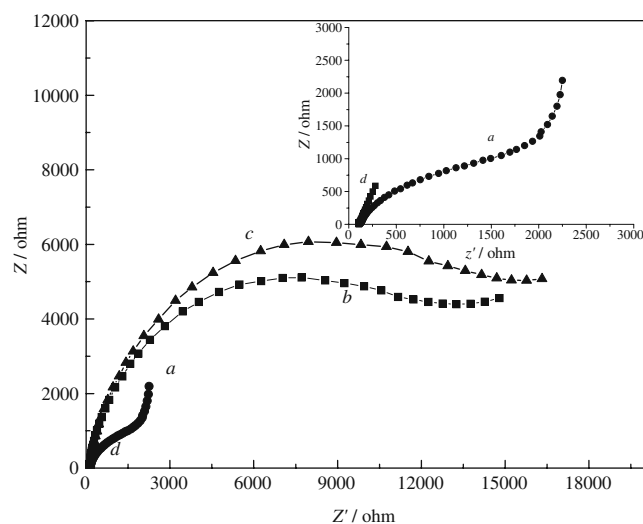


Fig. 2 EIS of MWCNTs-RTIL/GCE (a), the bare GCE (b), and RTIL/GCE (c), and MWCNTs/GCE (d) in 1.0 mM Fe(CN)₆^{3-/4-}+0.10 M KCl. The frequency range is 1–10⁵ Hz

Cyclic voltammetric behavior of QS

The cyclic voltammetric behaviors of 50 μM of QS at MWCNTs-RTIL/GCE, MWCNTs/GCE and the bared GCE had been investigated with the scanning rate of $50 \text{ mV}\cdot\text{s}^{-1}$ in 0.10 M of PBS over the potential range of 0–1.20 V as shown in curves of Fig. 3. From the curves in Fig. 3 it can be seen that a large and well-defined oxidation peak appears at 0.99 V at MWCNTs-RTIL/GCE, but there is a less sensitive electrochemical response of QS at the bared GCE and MWCNTs/GCE than that at MWCNTs-RTIL/GCE resulting from the synergetic effect of MWCNTs and RTIL.

The oxidation peak potential of QS at MWCNTs-RTIL/GCE slightly shifted to negative and the peak current increased by almost two times compared with that at MWCNTs/GCE and ten times compared with that at GCE, it means that the electrochemical oxidation of QS can be improved by MWCNTs-RTIL/GCE and the peak current enhancement is related not only to the increased electrode surface area, but also to both QS electrochemical oxidation process occurred easily at thermodynamically favorable potentials and the reaction rate increasing kinetically at MWCNTs-RTIL/GCE. On the one hand, MWCNTs with nano-scaled dimensions have a particular electronic structure, high electrical conductivity, and topological defects present on their surfaces which can be readily and completely used as an electrochemical sensing unit, yielding a higher sensitivity, and can bear both basal plane sites and the edge plane like sites/defects in their structures which may have caused the electrocatalytic efficiency during the electro-oxidation process [62–64]. On the other hand, the MWCNTs are untangled after treated with the

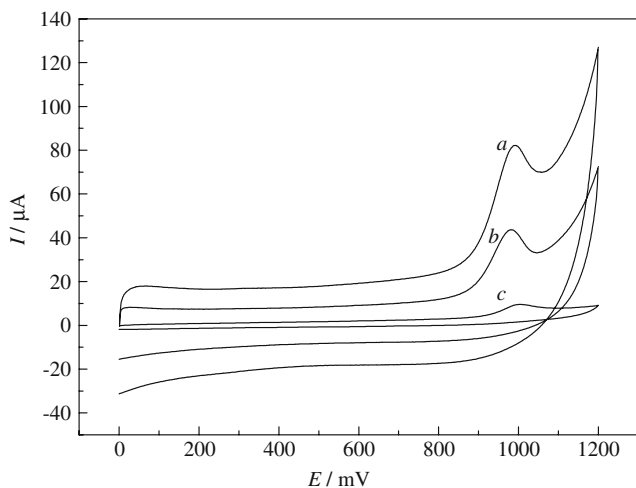


Fig. 3 CVs of 50 μM of QS at MWCNTs-RTIL/GCE (a), MWCNT/GCE (b), and GCE (c) in 0.10 M of PBS (pH 6.8). Scanning rate: $50 \text{ mV}\cdot\text{s}^{-1}$

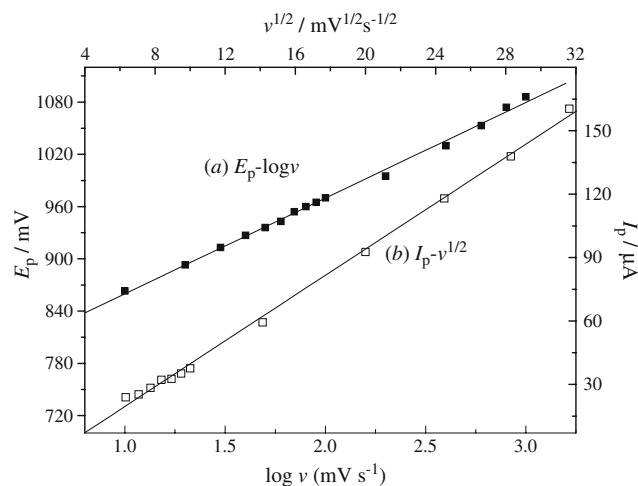


Fig. 4 a Dependence of the peak potentials on logarithm of scanning rates ($\log v$). b Dependence of the peak currents on the square roots of scanning rates ($v^{1/2}$)

RTIL, mainly because of cross-linking of the nanotube bundles mediated by local molecular ordering of RTIL resulting from the “cation- π ” interactions between imidazolium and nanotubes [19]. Therefore, MWCNTs-RTIL gel can act as a promoter to increase the heterogeneous electron transferring rate, and then produce the catalyzing QS electrochemical oxidation very well. In addition, no corresponding reduction peak was observed on the reverse scanning indicating the irreversibility of electrochemical oxidation.

The effect of scanning rate on the electrochemical behavior of 50 μM of QS at MWCNTs-RTIL/GCE was investigated by cyclic voltammetry (CV). With the potential sweeping rate increasing, both the peak currents increased and the peak potentials shifted positively which implied the irreversible nature of the electrode reaction processes. The oxidation peak currents versus the square roots of the scanning rate were a straight line shown in Fig. 4b, as expected for a diffusion-limited electrode reaction process. The linear regression equation is expressed as $I_{pa} (\mu\text{A}) = -14.57 + 5.428 v^{1/2} (\text{mV}^{1/2}\cdot\text{s}^{-1/2})$, with a correlation coefficient of 0.9990.

The effects of experimental conditions on the catalytic oxidation peak currents and the potentials

The effect of various media on the catalytic oxidation peak currents and potentials of QS could be easily observed from CV. The voltammetric behaviors of QS at scanning rate $50 \text{ mV}\cdot\text{s}^{-1}$ in different electrolytic solutions, such as aqueous NaCl, NaAc, NaNO_3 , Na_2SO_4 and NaAc-HAc, B-R, Na_2HPO_4 - NaH_2PO_4 (PBS) buffer solutions, had been investigated. The experimental results showed that in 0.10 M of aqueous PBS, QS had a well-defined electro-

chemical behavior. Thus, 0.10 M PBS was chosen as supporting electrolyte.

BMIMPF₆-MWCNT composite with different ratio was studied by CV in 50 μM of QS with 0.10 M PBS which indicated the peak currents of QS remained constant basically. However, when RTIL is too much or too little, they cannot form well paste for fabricating modified electrode. Their appropriate ratio is about 12/200 (mg/μL).

QS electrochemical oxidation is a pH-dependent one. The effect of solution pH on the oxidation peak current and peak potential for QS were studied in 0.10 M PBS over the range from pH 3.0 to 9.5 as shown in Fig. 5. From Fig. 5, it can be seen that with the increasing pH, the anodic peak potential shifted linearly to negative direction. The relationship between the anodic peak potential and the solution pH could be fit to the equation of $E_{pa}(mV) = -62.24 \text{ pH} + 1380.2$ (Fig. 5a), with a correlation coefficient of 0.9930. The slope was found to be -62.24 mV/pH , which was very close to the theoretical value of 59 mV, which indicated that the electron-transfer number and the number of protons taking part in the electrode reaction process was the same. Since the electrochemical oxidation of QS is known to occur by a two electron transfers [50], thus the number of protons involved were also predicted to be two. Figure 5b showed the dependence of the anodic peak current on the solution pH. It could be seen that the anodic current decreased with the increasing pH.

Electrochemical kinetics

Charge-transfer coefficient α

According to the results mentioned above, we knew that QS electrocatalytic oxidation was a diffusion-limited electrode reaction process. For an irreversible diffusion-controlled one, the peak potential (E_p) is proportional to the

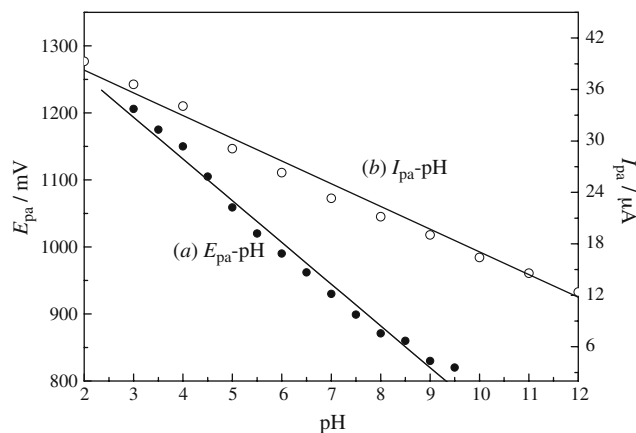


Fig. 5 Dependence of E_{pa} (a) and I_{pa} (b) on pH

logarithm of potential sweeping rate (ν) with the following equation [65]:

$$E_p = (b/2) \log \nu + constant \tag{1}$$

From the equation, we know that the slope of E_p vs. $\log \nu$ curve is $b/2$, where b indicates the Tafel slope. The dependency of E_p on $\log \nu$ for the oxidation of QS on the MWCNTs-RTIL/GCE is depicted in Fig. 4a, its linear regression equation is expressed as $E_p (mV) = 750.1 + 109.8 \log \nu$, with a correlation coefficient of 0.9984. A value of $b = 2 \times \partial E_p / \partial (\log \nu) = 219.7 \text{ mV}$ was obtained. From the equation $b = 2.3RT/n(1-\alpha)F$, we can calculate $n(1-\alpha) = 0.269$. As we know the electron transfer number of QS is 2 [50], so it gives the charge-transfer coefficient $\alpha = 0.87$.

The diffusion coefficient D

The real area of the electrode and the apparent diffusion coefficient of QS was determined by chronocoulometry (CC) [66].

$$Q = \frac{2nFACD^{1/2}t^{1/2}}{\pi^{1/2}} + Q_{dl} + Q_{ads} \tag{2}$$

Here, Q is the total charge, n is electron transferring number involved in the electrochemical oxidation reaction, A is the electrode surface area (cm^2), C is the concentration of the electroactive species in the solution (M), D is the diffusion coefficient ($\text{cm}^2 \cdot \text{s}^{-1}$), and t is the time (ms). The real area of the MWCNTs-RTIL/GCE were calculated to be 0.515 cm^2 from the slopes of Q vs. $t^{1/2}$ curves by using $5.0 \text{ mM Fe(CN)}_6^{3-}$ as model compound. As the number of electron transferring of QS is 2 [50], the real surface area (A) of MWCNTs-RTIL/GCE had been calculated before and the QS concentration (C) is $50 \text{ }\mu\text{M}$, the diffusion coefficient (D) of QS can be calculated to be $7.89 \times 10^{-3} \text{ cm}^2 \cdot \text{s}^{-1}$.

The electrode reaction rate constant k_f

The electrode reaction rate constant (k_f) can be determined by chronoamperometry (CA) using the following [67]:

$$I(t) = nFAk_f C [1 - 2H\sqrt{t}/\sqrt{\pi}] \tag{3}$$

in which, $H = k_f/D_{Ox}^{1/2} + k_b/D_{Rd}^{1/2}$. For the totally irreversible electrochemical reaction, the value of k_b is 0, therefore $H = k_f/D_{Ox}^{1/2}$. When t approaches to 0, the plot of $I(t)$ vs. $t^{1/2}$ gives a good straight line. Therefore, k_f can be calculated to be $3.43 \times 10^{-2} \text{ s}^{-1}$ from the slope and the intercept of CA curve.

Order number of the electrochemical reaction

According to the theory of the electrochemical kinetics [68], we obtained the dependence of the logarithm of the

peak current ($\log I_{pa}$) on the logarithm of QS concentration ($\log C_{QS}$). The logarithm of I_{pa} depends linearly on the logarithm of C_{QS} with a linear relationship equation of $\log I_{pa} = -0.4892 + 0.89541 \log C_{QS}$, and the correlation coefficient (R) of 0.9992. The slope is approximating to 1, which implies that the electrocatalytic oxidation reaction obeys the first-order kinetics with respect to QS.

In order to check the electrochemical response of MWCNTs-RTIL/GCE for QS, the time-steady state current response curve was determined and the experimental results are shown in Fig. 6. The current response signal of MWCNTs-RTIL/GCE is proportional to QS concentration, response time is less than 4 s, and the least response concentration is 0.4 μM which can be used in QS electrochemical quantitative determination with both low detection limit and high sensitivity.

Electrochemical determination application

Operational parameters optimization of the square wave voltammetry

The square wave voltammetry response markedly depends on the parameters of the excitement signals. Therefore, optimization of pulse amplitude, frequency, and the scanning potential increment were investigated in the experiment. The dependence of the oxidation peak current on pulse amplitude was examined in the range 10–100 mV. Between 10 and 50 mV, the variation of the peak currents with the pulse amplitude was a linear increasing, after 50 mV the variations remained almost constant. Thus, a pulse amplitude of 50 mV was chosen to improve the sensitivity without peak distortion. With a 50 mV pulse amplitude, the frequency was varied in the range 2–24 Hz. From the experimental results, we found that between 5 and

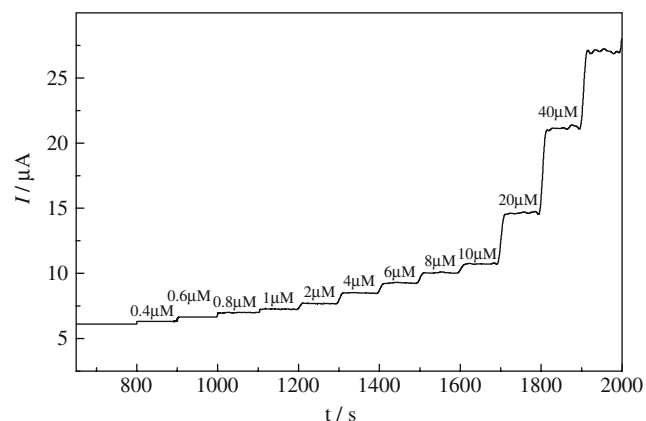


Fig. 6 Time-dependent steady state currents obtained at MWCNTs-RTIL/GCE while increasing QS concentration at 1.05 V with a stirring rate of 100 rpm

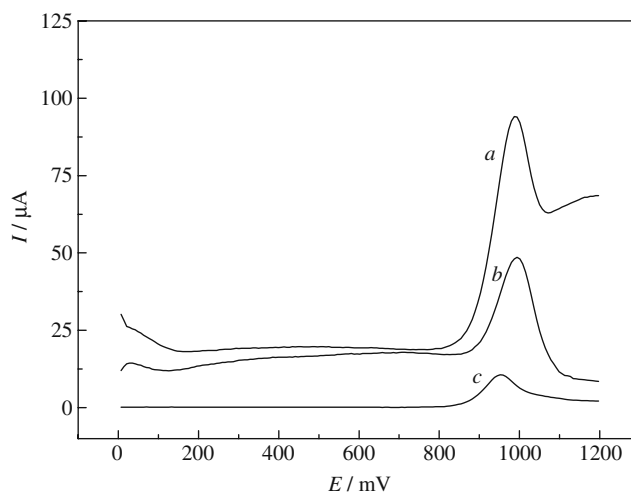


Fig. 7 SWVs of 50 μM of QS at MWCNTs-RTIL/GCE (a), MWCNTs-GCE (b), and GCE (c) in 0.10 M of PBS (pH 6.8)

12 Hz, the peak current increased linearly with increasing frequency; after 12 Hz, the variation of the current with the frequency remained almost constant. A value of 12 Hz was chose. Also with a 50-mV pulse amplitude and a 12 Hz frequency, a scanning potential increment of 7 mV was found to develop a well-defined peak and a higher current response. Lower or higher than 7 mV, the peak current was decreased.

Square-wave voltammetric behaviors of QS electrocatalytic oxidation

The square wave voltammetry (SWV) behaviors of 50 μM QS at MWCNTs-RTIL/GCE, MWCNT/GCE, and GCE in 0.10 M PBS under the optimized experimental conditions (amplitude 50 mV, frequency 12 Hz, and scanning potential increment 7 mV) was shown in Fig. 7. From the curves of Fig. 7, it can be seen that QS itself showed a sluggish SWV response at the bared GCE and a less sensitive electrochemical response at MWCNTs/GCE in contrast to that at MWCNTs-RTIL/GCE, which revealed a faster electron transfer process of QS at MWCNTs-RTIL/GCE. The experimental result was in quite good agreement with that of CV.

The electrocatalytic oxidation peak currents for QS with the variation of its concentrations were investigated at MWCNTs-RTIL/GCE. Linear calibration curves are obtained over the concentration ranges of 3.0 μM –0.10 mM in 0.10 M PBS (pH 6.8) with a linear fitting regression equation of $I_{pa}(\mu\text{A}) = 2.632 + 824.48 C_{QS}(\text{mM})$ and a correlation coefficient of 0.9989. The detection limit was 0.44 μM for QS according to $S/N=3$ ($n=10$). Under the optimized experimental conditions, the direct determination of 50 μM QS in 0.10 M PBS was checked in the presence of some common compounds or ions found in

pharmaceutical preparations. The determination results showed that within a relative error of $\pm 5\%$, 1,000-fold of inorganic ions K^+ , Na^+ , Cl^- , NO_3^- , SO_4^{2-} , and the 50-fold of glucose, saccharose and citrate do not affect QS current response which suggested that the proposed voltammetric method had excellent selectivity toward QS.

In order to examine the reproducibility of MWCNTs-RTIL/GCE, ten times of the determination was performed by one MWCNTs-RTIL/GCE; nearly the same results were obtained. A relative standard deviation of 4.7% was obtained by measuring the oxidation peak current for QS electrochemical oxidation with cyclic voltammetry using six independent MWCNTs-RTIL/GCE. The experimental results showed a good reproducibility for the modified electrode.

Determination of quinine in commercial quinine dihydrochloride injection sample

The proposed methods were successfully applied in the determination of a quinine in commercial injection sample. The proposed method afforded $250 \text{ mg}\cdot\text{mL}^{-1}$ with relative standard deviations of 1.37–2.85%, based on the average of the six repeated measurements. The accuracy of the proposed method was also judged by applying the standard addition, and their mean percentage recoveries are 96.20–100.3%. This determination results implied that there were no significant differences between the proposed and the reported conventional method with respect to reproducibility, accuracy, and precision. In other words, the proposed method provides a convenient and efficient one for the determination of quinine with the advantages of simplicity, sensitivity, and the rapidity.

Conclusion

The electrochemical behaviors, electrochemical kinetics, and electrochemical determination of quinine sulfate were performed for the first time by several electrochemical methods based on the application of the MWCNTs-RTIL/GCE. A well-defined irreversible electrocatalytical oxidation peak was obtained. The QS electrocatalytical oxidation reaction at MWCNTs-RTIL/GCE is a diffusion-controlled process involving two electrons transferring accompanied by two protons taking part in the electrode reaction process. Meanwhile, the electrochemical kinetic parameters (charge transfer coefficient α , diffusion coefficient D , and the electrode reaction rate constant k_f) were determined by CC and CA, which could provide some help in the insight into quinine metabolic fate in redox processes, pharmacological activity [69–72] and had an impact on drug pharmacokinetics and pharmacodynamics. From the recovery deter-

mined results, a good accuracy and precision of the proposed method was obtained. Therefore, it can be concluded that the proposed voltammetric method is simpler, cheaper, less time-consuming, less toxicity, and more easy to apply than the non-aqueous titration, chromatography, chemiluminescence, flow injection analysis, fluorodensitometric methods and fluorimetry, and polarography. However, the disadvantage of the proposed methods is that it cannot be directly applied for the selective and simultaneous determination of QS with other alkaloids in complex samples.

Acknowledgments This work was financially supported by Key Research Project of Education Ministry of Ningxia (No.200623).

References

- Lijima S (1991) *Nature* 354:56–58
- Ajayan PM (1999) *Chem Rev* 99:1787–1799
- Odom TW, Huang JL, Kim P, Lieber CM (1998) *Nature* 391:62–64
- Jang JW, Lee DK, Lee CE, Lee TJ, Lee CJ, Noth SJ (2002) *Solid State Commun* 122:619–622
- Tekleab D, Czerw R, Carroll DL, Ajayan PM (2000) *Appl Phys Lett* 76:3594–3596
- Nugent JM, Santhanam KSV, Rubio A, Ajayan PM (2001) *Nano Lett* 1:87–91
- Dai X, Wildgoose GG, Compton RG (2006) *Analyst* 131:901–906
- Hu C, Chen X, Hu S (2006) *J Electroanal Chem* 586:77–85
- Antiochia R, Lavagnini I (2006) *Anal Lett* 39:1643–1655
- Ricci F, Amine A, Moscone D, Moscone D (2003) *Anal Lett* 36:1921–1938
- Moulthrop JS, Swatloski RP, Moyna G, Rogers RD (2005) *Chem Commun* 12:1557–1559
- Luo HM, Dai S, Bonnesen PV, Buchanan AC, Holbery JD, Bridges NJ, Rogers RD (2004) *Anal Chem* 76:3078–3083
- Welton T (1999) *Chem Rev* 99:2071–2083
- Kosmulski M, Osteryoung RA, Ciszowska M (2000) *J Electrochem Soc* 147:1454–1458
- Yu P, Lin YQ, Xiang L, Su L, Zhang J, Mao LQ (2005) *Langmuir* 21:9000–9006
- Wassercheid P, Keim W (2000) *Angew Chem Int Ed* 39:3772–3789
- Rantwijk V, Lau F, Sheldon RM (2003) *Trends Biotechnol* 21:131–138
- Huddleston JG, Willauer HD, Swatloski RP, Visser AE, Rogers RD (1998) *Chem Commun* 16:1765–1766
- Fukushima T, Kosaka A, Ishimura Y, Yamamoto T, Takigawa T, Ishii N, Aida T (2003) *Science* 300:2072–2074
- Zhao Q, Zhan DP, Ma HY, Zhang MQ, Zhao YF, Jing P, Zhu ZW, Wan XH, Shao YH, Zhuang QK (2005) *Front Biosci* 10:326–334
- Liu LQ, Zhao FQ, Xiao F, Zeng BZ (2008) *Electroanalysis* 20:2148–2152
- Liu Y, Liu L, Dong SJ (2006) *Electroanalysis* 19:55–59
- Stork G, Niu D, Fujimoto A, Koft ER, Balkovec JM, Tata JR, Dake GR (2001) *J Am Chem Soc* 123:3239–3242
- Garcia Castro JC, Sanchez MJ, Rodriguez Delgado MA, Romero CD (1993) *Mikrochim Acta* 110:263–268
- Baroni A, Paoletti I, Ruocco E, Ayala F, Corrado F, Wolf R, Tufano MA, Donnarumma G (2007) *J Dermatol Sci* 47:253–255
- Wolf R, Wolf D, Ruocco V (2000) *Clin Dermatol* 18:17–35

27. Paton NI, Aboulhab J (2005) *HIV Med* 6:13–20
28. State Pharmacopoeia Commission of the People's Republic of China (Eds) (2005) *Pharmacopoeia of the People's Republic of China*, vol II. Chemical Industry Press, Beijing, pp 744
29. Li B, Zhang Z, Wu M (2000) *Talanta* 51:515–522
30. Koukli IL, Calokerinos AC (1990) *Anal Chim Acta* 236:463–468
31. Reijenga JC, Aben GVA, Lemmens AAG, Verheggen TPEM, De Bruijn CHMM, Everaerts FM (1985) *J Chromatogr A* 320:245–252
32. Beljaars PR, Koken PJ (1972) *J Assoc Off Anal Chem* 56:1284–1291
33. Ortega Algar S, Ramos Martos N, Molina diaz A (2004) *Microchim Acta* 147:211–217
34. Gong ZL, Zhang ZJ (1997) *Fresenius J Anal Chem* 357:1093–1096
35. Nuijens JM, van der Velden H (1973) *Z Lebensm Unters Forsch* 153:97–98
36. van Gils WF, Hidskes GG (1972) *Z Lebensm Unters Forsch* 148:89–91
37. Yebra MC, Cespon RM (2000) *Microchem Journal* 65:81–86
38. Issa YM, Ibrahim H, Shoukry AF, Mohamed SK (1995) *Mikrochim Acta* 118:257–263
39. Wang XR, Li GH, Tang QH, Pan LL, Fan SY (2004) *Chin J Anal Chem (Ch)* 32:1083–1085
40. Garcia Castro JC, Sanchez MJ, Delgado MAR, Romero CD (1993) *Mikrochim Acta* 110:263–268
41. Soyinka JO, Onyeji CO, Omoruyi SI (2009) *J Chromatogr B* 877:441–445
42. Damien R, Daval S, Souweine B, Deteix P, Eschaliere A, Coudore F (2006) *Rapid Commun Mass Spectrom* 20:2528–2532
43. Mirghani RA, Ericsson O, Cook J, Yu P, Gustafsson LL (2001) *J Chromatogr B Biomed Sci Appl* 754:57–64
44. Dua VK, Sarin R, Prakash A (1993) *J Chromatogr* 614:87–93
45. Kolawole JA, Mustapha A (2000) *Biopharm & Drug Dispos* 21:345–352
46. Jeuring HJ, van den Hoeven W, van Doorninck P, ten Broeke R (1979) *Z Lebensm Unters Forsch* 169:281–283
47. Ibrahim H, Bouajila J, Siri N, Rozing G, Nepveu F, Couderc F (2007) *J Chromatogr B* 850:481–487
48. Chaulet JF, Robet Y, Prevosto JM, Soares O, Brazier JL (1993) *J Chromatogr* 613:303–310
49. Thomas FG, Gierst L (1983) *J Electroanal Chem* 154:239–260
50. Kobayashi Y, Martin CR (1999) *Anal Chem* 71:3665–3672
51. Li DH, Ding YD (1995) *Chin J Anal Chem (Ch)* 23:1271–1273
52. Zareh MM, Malinowska E, Kasiura K (2001) *Anal Chim Acta* 447:55–61
53. Saad B, Bee-Leng Y, Saleh MI, Rahman IA, Mansor SM (2001) *J Assoc Off Anal Chem* 84:1151–1157
54. Liu LH, Gao ZN (2010) *Chin J Pharm Anal (Ch)* 30:83–87
55. Sun YQ, You W, Gao ZN (2008) *Acta Pharm Sin (Ch)* 43:396–401
56. Gao ZN, Sun YQ, You W (2009) *Chin J Anal Chem (Ch)* 37:553–557
57. Zhan XM, You W, Gao ZN (2009) *Chin J Pharm Anal (Ch)* 29:1543–1546
58. Tsang SC, Chen YK, Harris PJF, Green MLH (1994) *Nature* 372:159–162
59. Feng JJ, Zhao G, Xu JJ, Chen HY (2005) *Anal Biochem* 342:280–286
60. Xiang CL, Zou YJ, Sun LX, Xu F (2008) *Electrochem Commun* 10:38–41
61. Barsoukov E, Macdonald JR (eds) (2005) *Impedance spectroscopy: theory, experiment, and applications*, 2nd edn. Wiley, New Jersey
62. Britto PJ, Santhanam KSV, Rubio A, Alonso A, Ajayan PM (1999) *Adv Mater* 11:154–157
63. Musameh M, Lawrence NS, Wang J (2005) *Electrochem Commun* 7:14–18
64. Banks CE, Compton RG (2006) *Analyst* 131:15–21
65. Golabi SM, Zare HR (1999) *Electroanalysis* 11:1297–1298
66. Adams RN (1969) *Electrochemistry at solid electrode*. Marcel Dekker Inc, New York, pp 220–222
67. Wu HQ, Li YF (1998) *Electrochemical kinetics*. China Higher Education Press, Beijing and Springer, Verlag Berlin Heidelberg, pp 96–100
68. Wu HH (2004) *Electrochemistry*. Chemical Industry, Beijing, pp 84–85
69. Wang J (ed) (1996) *Electroanalytical techniques in clinical chemistry and laboratory medicine*. VCH, New York
70. Kissinger PT, Heineman WR (eds) (1996) *Laboratory techniques in electroanalytical chemistry*, 2nd edn. Marcel Dekker Inc, New York
71. Ozkan SA, Uslu B, Aboul-Enein HY (2003) *Crit Rev Anal Chem* 33:155–181
72. Smyth MR, Vos JG (eds) (1992) *In analytical voltammetry*. Elsevier Science Ltd, Amsterdam